

Unified pictures of Q-balls and Q-tubes

Takashi Tamaki*

*Department of Physics, General Education, College of Engineering,
Nihon University, Tokusada, Tamura, Koriyama, Fukushima 963-8642, Japan*

Nobuyuki Sakai†

Department of Education, Yamagata University, Yamagata 990-8560, Japan

While Q-balls have been investigated intensively for many years, another type of nontopological solutions, Q-tubes, have not been understood very well. In this paper we make a comparative study of Q-balls and Q-tubes. First, we investigate their equilibrium solutions for four types of potentials. We find, for example, that in some models the charge-energy relation is similar between Q-balls and Q-tubes while in other models the relation is quite different between them. To understand what determines the charge-energy relation, which is a key of stability of the equilibrium solutions, we establish an analytical method to obtain the two limit values of the energy and the charge. Our prescription indicates how the existent domain of solutions and their stability depends on their shape as well as potentials, which would also be useful for a future study of Q-objects in higher-dimensional spacetime.

PACS numbers: 03.75.Lm, 11.27.+d

I. INTRODUCTION

Among nontopological solitons, Q-balls have attracted much attention because they can exist in all supersymmetric extensions of the Standard Model [1]. Specifically, they can be produced efficiently in the Affleck-Dine (AD) mechanism [2] and could be responsible for baryon asymmetry [3] and dark matter [4]. Q-balls can also influence the fate of neutron stars [5]. Based on these motivations, stability of Q-balls has been intensively studied [6–9].

In spite of these concerns about Q-balls, other equilibrium solutions have not been studied so much, while topological defects have several types according to the symmetry. For example, observational consequences by cosmic strings, such as gravitational lenses and the gravitational wave have been argued for years [10].

From this point of view, other types of nontopological solutions may play an important role in the universe. Recently, two types of nontopological solutions was discussed: Q-tubes and Q-crust, which mean tube-shaped (or string-like) and crust-shaped solutions, respectively [11]. As for Q-tubes, some numerical studies manifested sign of their appearance. First, it has been reported that a filament structure appears just before Q-ball formation in the numerical simulations [12]. Second, according to the simulations of the collision of two Q-balls, two apparent rings are formed [13]. We conjecture that the filament structure and the rings are Q-tubes.

In [11] numerical solutions were investigated for the potential,

$$V_3(\phi) := \frac{m^2}{2}\phi^2 - \mu\phi^3 + \lambda\phi^4 \quad \text{with } m^2, \mu, \lambda > 0, \quad (1)$$

which we call the V_3 model. In the case of Q-balls [6–8], however, the charge-energy relation, which is a key of stability of the equilibrium solutions, is quite dependent on potentials $V(\phi)$. Therefore, our first concern is how Q-tube solutions depend on potentials.

Our second concern is how different in the charge-energy relation between Q-tubes and Q-balls. This shape-dependence is closely related to the dimension-dependence because a cylindrical Q-tube in 3+1 spacetime is equivalent to a “Q-ball” in 2+1 spacetime if we ignore gravity. If this dimension-dependence becomes manifest, it would be useful for investigating other Q-objects or those in higher-dimensional spacetime [14].

For these reasons, in this paper, we make a comparative study of Q-balls and Q-tubes. This paper is organized as follows. In Sec. II, we explain briefly what Q-balls and Q-tubes are. In Sec. III, we investigate their equilibrium solutions numerically for four types of potentials. In Sec. IV, we evaluate analytically the limit values of the energy and the charge. In Sec. V, we devote to concluding remarks.

II. EQUILIBRIUM SOLUTIONS

Consider an $SO(2)$ -symmetric scalar field $\phi = (\phi_1, \phi_2)$, whose action is given by

$$S = \int d^4x \left[-\frac{1}{2}\eta^{\mu\nu}\partial_\mu\phi \cdot \partial_\nu\phi - V(\phi) \right], \quad \phi \equiv \sqrt{\phi \cdot \phi}. \quad (2)$$

*Electronic address: tamaki@ge.ce.nihon-u.ac.jp

†Electronic address: nsakai@e.yamagata-u.ac.jp

A. Q-balls

For a Q-ball, we assume spherical symmetry and homogeneous phase rotation,

$$\phi = \phi(r)(\cos \omega t, \sin \omega t). \quad (3)$$

One has a field equation,

$$\frac{d^2 \phi}{dr^2} + \frac{2}{r} \frac{d\phi}{dr} + \omega^2 \phi = \frac{dV}{d\phi}. \quad (4)$$

This is equivalent to the field equation for a single static scalar field with an effective potential

$$V_\omega = V - \frac{1}{2} \omega^2 \phi^2. \quad (5)$$

Equilibrium solutions $\phi(r)$ with a boundary condition

$$\frac{d\phi}{dr}(r=0) = 0, \quad \phi(r \rightarrow \infty) = 0, \quad (6)$$

exist if $\min(V_\omega) < V_\omega(0)$ and $d^2 V_\omega / d\phi^2(0) > 0$. This condition is rewritten as

$$\min \left[\frac{2V}{\phi^2} \right] < \omega^2 < m^2 \equiv \frac{d^2 V}{d\phi^2}(0), \quad (7)$$

where we have put $V(0) = 0$ without loss of generality.

For a Q-ball solution, we can define the energy and the charge, respectively, as

$$E = 4\pi \int_0^\infty r^2 dr \left\{ \frac{1}{2} \omega^2 \phi^2 + \frac{1}{2} \left(\frac{d\phi}{dr} \right)^2 + V \right\},$$

$$Q = 4\pi \omega \int_0^\infty r^2 \phi^2 dr. \quad (8)$$

The Q - E relation is a key to understand stability of equilibrium solutions in terms of catastrophe theory [8].

B. Q-tubes

For a Q-tube, we suppose a string-like configuration,

$$\phi = \phi(R)(\cos(n\varphi + \omega t), \sin(n\varphi + \omega t)), \quad (9)$$

where n is nonnegative integer and (R, φ, z) is the cylindrical coordinate system. The field equation becomes

$$\frac{d^2 \phi}{dR^2} + \frac{1}{R} \frac{d\phi}{dR} - \frac{n^2 \phi}{R^2} + \omega^2 \phi = \frac{dV}{d\phi}. \quad (10)$$

In the case of $n = 0$, the field equation is the same as (4) except for a numerical coefficient. Therefore, Q-ball-like solutions of $\phi(R)$ exist if the condition (7) is satisfied.

In the case of $n \geq 1$, there is no regular solution which satisfies $\phi(0) \neq 0$. However, if we adopt a different boundary condition,

$$\phi(R=0) = \phi(R \rightarrow \infty) = 0, \quad (11)$$

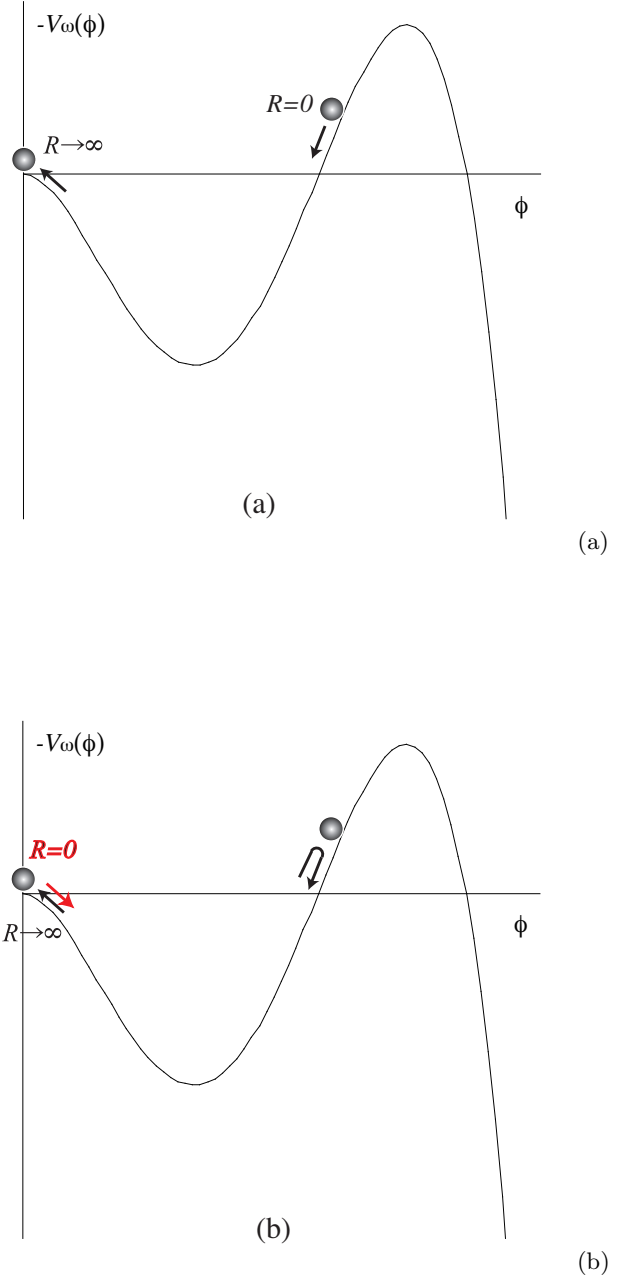


FIG. 1: Interpretation of (a) Q-balls and $n = 0$ solutions in Q-tubes and (b) $n \geq 1$ solutions in Q-tubes by analogy with a particle motion in Newtonian mechanics.

there is a new type of regular solutions. We introduce an auxiliary variable ψ which is defined by $\phi(R) = R^n \psi(R)$. Then, Eq.(10) becomes

$$\frac{d^2 \psi}{dR^2} + \frac{2n+1}{R} \frac{d\psi}{dR} + \omega^2 \psi = R^{-n} \frac{dV}{d\phi} \Big|_{\phi=R^n \psi} \quad (12)$$

	lower limit of ω^2	upper limit of ω^2
Type I: $\min[V] = 0$	$\min[2V/\phi^2]$ (thin)	m^2 (thick)
Type II: $\min[V] < 0$	0	m^2 (thick)

TABLE I: Two types of Q-balls/Q-tubes solutions and two limits of ω^2 .

If we choose $\psi(0)$ appropriately, we obtain a solution $\psi(R)$ which is expressed in the Maclaurin series without odd powers in the neighborhood of $R = 0$. In terms of the original variable $\phi(R)$, the n th differential coefficient $\phi^{(n)}(0) = \psi(0)$ should be determined by the shooting method, while any lower derivative vanishes at $R = 0$.

In the same way as for Q-balls [15], existence of Q-tube solutions can be interpreted as follows. If one regards the radius R as ‘time’ and the scalar amplitude $\phi(R)$ as ‘the position of a particle’, one can understand $n = 0$ solutions in words of Newtonian mechanics, as shown in Fig. 1(a). Equation (10) describes a one-dimensional motion of a particle under the conserved force due to the potential $-V_\omega(\phi)$ and the ‘time’-dependent friction $-(1/R)d\phi/dR$. If one chooses the ‘initial position’ $\phi(0)$ appropriately, the static particle begins to roll down the potential slope, climbs up and approaches the origin over infinite time.

Similarly, we can also understand $n \geq 1$ solutions as shown in Fig. 1(b). In this case, there are two non-conserved forces, the friction $-(1/R)d\phi/dR$ and the repulsive force $n^2\phi^2/R^2$. If $n = 1$, by choosing the ‘initial velocity’ $d\phi/dR(0)$ appropriately, the particle goes down and up the slope, and at some point $\phi = \phi_{\max}$ it turns back and approaches the origin over infinite time. If $n \geq 2$, $d\phi/dR(0)$ vanishes; instead, the n th derivative $\phi^{(n)}(0)$ gently pushes the particle at $\phi = 0$. Therefore, with the appropriate choice of $\phi^{(n)}(0)$, the particle moves along a similar trajectory to that of $n = 1$. This argument also indicates that the existence condition of $n \geq 1$ solutions are the same as that of $n = 0$ solutions, (7). Solutions with the same behavior as the $n = 1$ solutions were obtained by Kim *et al.*[16], who studied the SO(3)-symmetric scalar field without Q-charge.

Because our Q-ball solutions are infinitely long, the energy and the charge (8) diverge. We therefore define the energy and the charge per unit length, respectively, as

$$e = 2\pi \int_0^\infty R dR \left\{ \frac{1}{2}\omega^2\phi^2 + \frac{1}{2} \left(\frac{d\phi}{dR} \right)^2 + \frac{n^2\phi^2}{2R^2} + V \right\},$$

$$q = 2\pi\omega \int_0^\infty R\phi^2 dR. \quad (13)$$

C. Two types and two limits

The existence condition (8) indicates that both Q-balls and Q-tubes are classified into two types of solutions, according to the sign of $\min[V(\phi)]$.

Type I: $\min[V(\phi)] = V(0) = 0$. In this case $\min[2V/\phi^2]$ is also positive and the lower limit of ω . The two limits $\omega^2 \rightarrow \min[2V/\phi^2]$ and $\omega^2 \rightarrow m^2$ correspond to the thin-wall limit and the thick-wall limit, respectively.

Type II: $\min[V(\phi)] < 0$. In this case $\min[2V/\phi^2]$ is negative. Because $\omega^2 > 0$, there is no thin-wall limit, $\omega^2 \rightarrow \min[2V/\phi^2]$. The thick-wall limit, $\omega^2 \rightarrow m^2$, still exists.

The two limits of ω^2 for the two types of solutions are summarized in Table I.

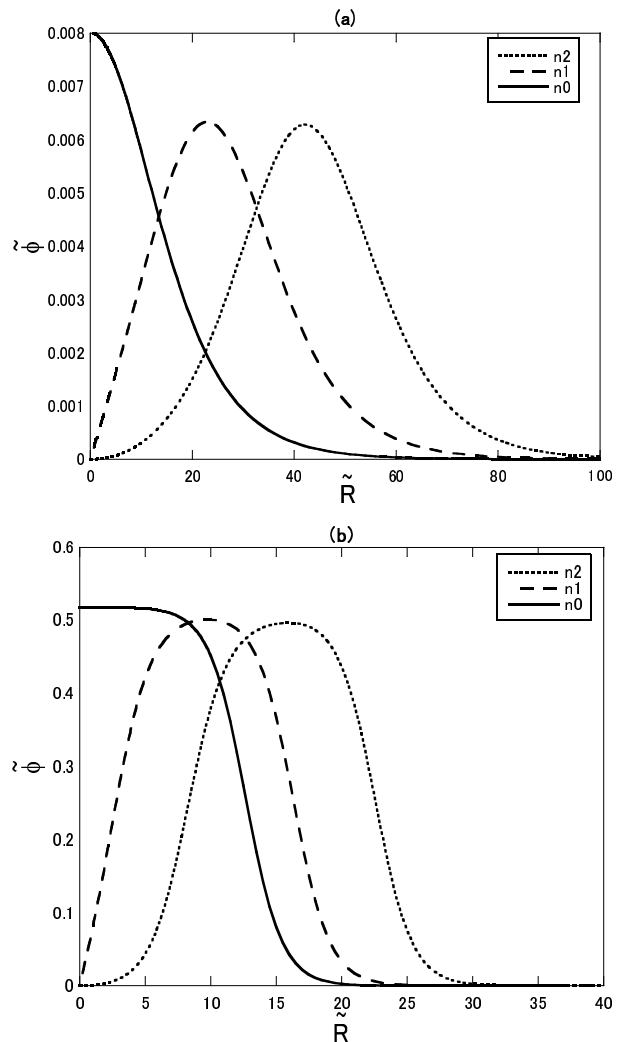


FIG. 2: The field configurations of the scalar field for Q-tubes in the V_3 model with $\tilde{m}^2 = 0.6$ (Type I): (a) $\epsilon^2 = 0.01$ (thick-wall) and $\epsilon^2 = 0.48$ (thin-wall).

III. SOLUTIONS IN VARIOUS POTENTIALS

Here we investigate equilibrium solutions of Q-balls and Q-tubes for four types of potentials.

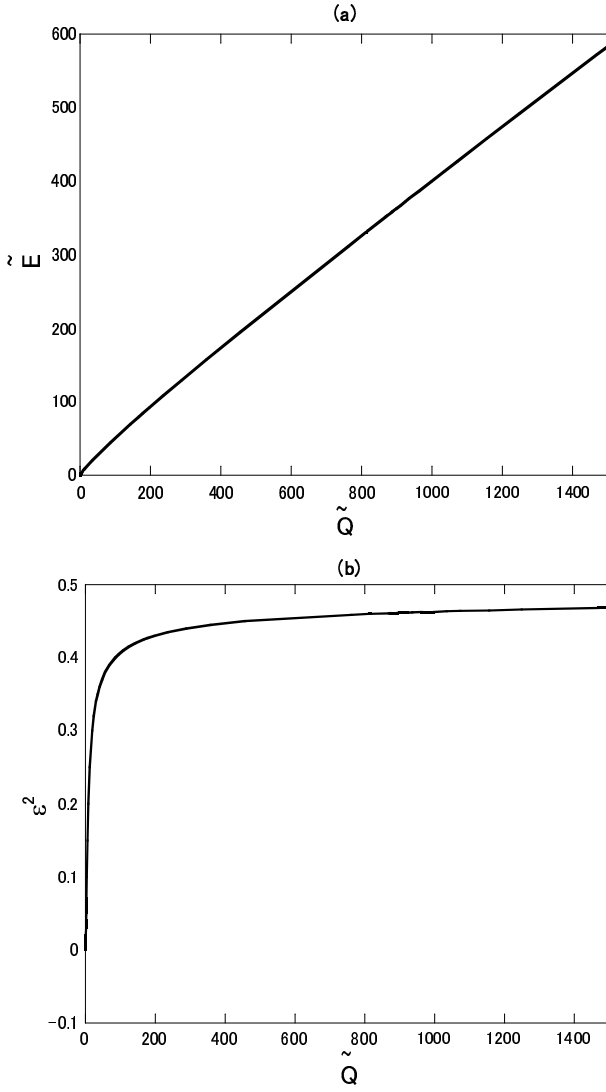


FIG. 3: (a) \tilde{Q} - \tilde{E} and (b) \tilde{Q} - ϵ^2 relations for Type I Q-balls in the V_3 model: $\tilde{m}^2 = 0.6$.

A. V_3 model

First, we summarize the previous results in the V_3 model (1) [11]. We rescale the quantities as

$$\begin{aligned}\tilde{\phi} &\equiv \frac{\lambda}{\mu}\phi, \quad \tilde{m} \equiv \frac{\sqrt{\lambda}}{\mu}m, \quad \tilde{\omega} \equiv \frac{\sqrt{\lambda}}{\mu}\omega, \\ \tilde{r} &\equiv \frac{\mu}{\sqrt{\lambda}}r, \quad \tilde{E} \equiv \frac{\lambda^{3/2}}{\mu}E, \quad \tilde{Q} \equiv \lambda Q, \\ \tilde{R} &\equiv \frac{\mu}{\sqrt{\lambda}}R, \quad \tilde{e} \equiv \frac{\lambda^2}{\mu^2}e, \quad \tilde{q} \equiv \frac{\lambda^{3/2}}{\mu}q,\end{aligned}\quad (14)$$

and define a parameter,

$$\epsilon^2 \equiv \tilde{m}^2 - \tilde{\omega}^2. \quad (15)$$

Then, the existing condition (7) for the two types be-

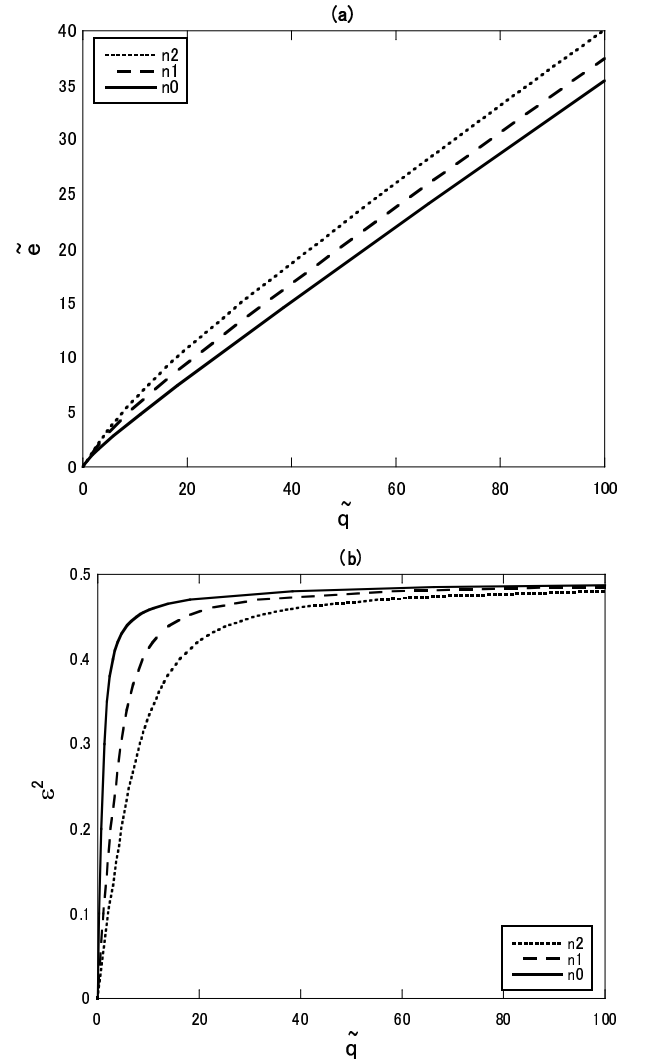


FIG. 4: (a) \tilde{q} - \tilde{e} and (b) \tilde{q} - ϵ^2 relations for Type I Q-tubes in the V_3 model: $\tilde{m}^2 = 0.6$.

comes

$$\begin{aligned}0 < \epsilon^2 < \frac{1}{2} &\text{ for } \tilde{m}^2 > \frac{1}{2} \text{ (Type I)} \\ 0 < \epsilon^2 < \tilde{m}^2 &\text{ for } \tilde{m}^2 < \frac{1}{2} \text{ (Type II)}.\end{aligned}\quad (16)$$

The limits $\epsilon^2 \rightarrow 1/2$ and $\epsilon^2 \rightarrow 0$ correspond to the thin-wall limit and the thick-wall limit, respectively. As we discussed in the last section, however, in Type II solutions there is no thin-wall limit and the upper limit of ϵ^2 is \tilde{m}^2 instead of $1/2$.

Figure 2 shows examples of the field configurations of Q-tubes. We fix $\tilde{m}^2 = 0.6$ (Type I), and choose $\epsilon^2 = 0.01$ (thick-wall) in (a) and $\epsilon^2 = 0.48$ (thin-wall) in (b). In each diagram we show the three solutions $n = 0, 1$ and 2 , which indicates that the maximum amplitude of the scalar field ϕ_{\max} for $n = 0$ is largest among them. We can understand it by analogy with the Newtonian mechanics in Fig. 1. For $n \geq 1$, the particle must make a

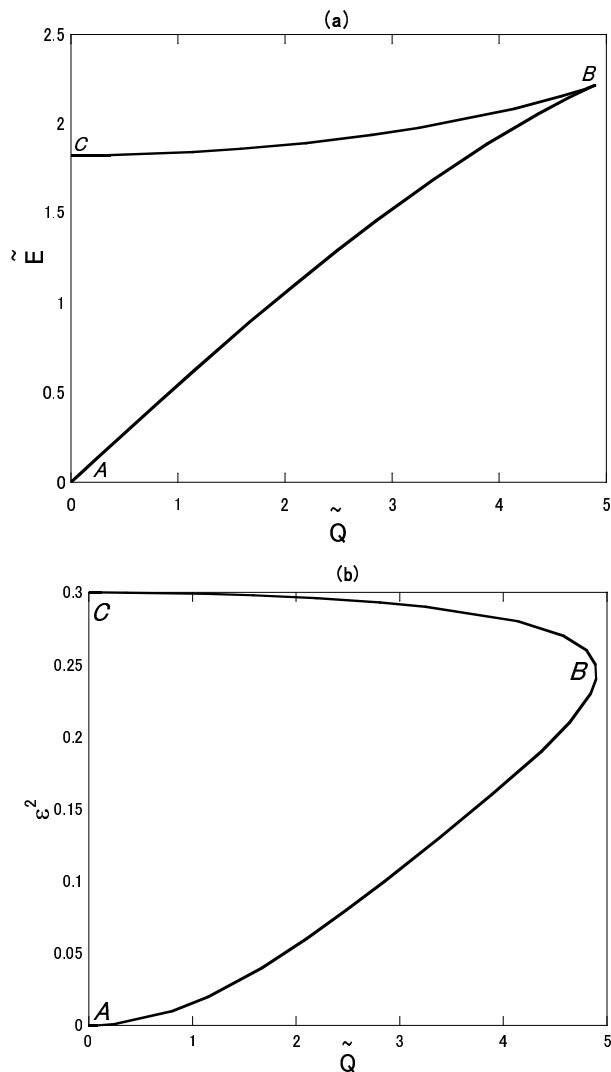


FIG. 5: (a) \tilde{Q} - \tilde{E} and (b) \tilde{Q} - ϵ^2 relations for Type I Q-balls in the V_3 model: $\tilde{m}^2 = 0.3$.

round trip while it goes an one-way for $n = 0$. Nevertheless, $\tilde{\phi}_{\max}$ in all cases are qualitatively unchanged which means that the conservation law of energy approximately holds in words of the Newtonian mechanics. Of course, the behavior of a Q-ball is similar to that of a Q-tube for $n = 0$. These properties are independent of potentials, which is important in understanding Q-balls and Q-tubes in an unified way as we shall see in Sec. IV.

We show the charge-energy- ϵ relations for Type I ($\tilde{m}^2 = 0.6$): Q-balls in Fig. 3 and Q-tubes in Fig. 4. As for Q-tubes, we show results for $n = 0, 1$ and 2 . Similarity between Q-balls and Q-tubes is quite remarkable. In the thin-wall limit ($\epsilon^2 \rightarrow 1/2$), we confirm that \tilde{Q} , \tilde{E} , \tilde{q} and \tilde{e} diverge. In the thick-wall limit ($\epsilon^2 \rightarrow 0$), on the other hand, these quantities approach zero.

We also show the same relations for Type II ($\tilde{m}^2 = 0.3$): Q-balls in Fig. 5 and Q-tubes in Fig. 6. The crucial difference from Type I is that \tilde{Q} and \tilde{q} approach zero in

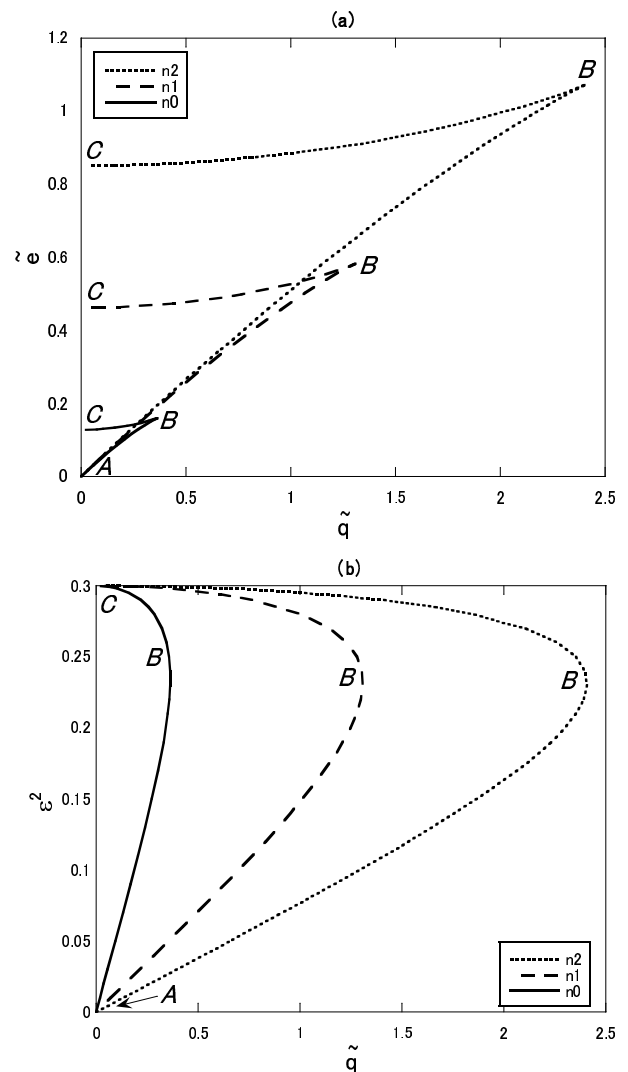


FIG. 6: (a) \tilde{q} - \tilde{e} and (b) \tilde{q} - ϵ^2 relations for Type I Q-tubes in the V_3 model: $\tilde{m}^2 = 0.3$.

the upper limit $\epsilon^2 \rightarrow \tilde{m}^2$ while \tilde{E} and \tilde{e} have nonzero finite values corresponding to the points C . As a result, \tilde{Q} , \tilde{E} , \tilde{q} and \tilde{e} have maximum values for intermediate value of ϵ^2 corresponding to the points B where cusp structures appear in Figs. 5 and 6 (a). The stability of Q-balls and Q-tubes can be understood using catastrophe theory [17]. Solutions from the point A to B is stable while B to C unstable.

The extreme values of the energy and the charge of Q-balls and Q-tubes in the V_3 model are summarized in Table II.

	$\epsilon^2 \rightarrow \min[1/2, \tilde{m}^2]$	$\epsilon^2 \rightarrow 0$ (thick)
Type I: $\tilde{m}^2 > 1/2$	$\tilde{E}, \tilde{Q}, \tilde{e}, \tilde{q} \rightarrow \infty$	$\tilde{E}, \tilde{Q}, \tilde{e}, \tilde{q} \rightarrow 0$
Type II: $\tilde{m}^2 < 1/2$	$\tilde{E}, \tilde{e} \rightarrow \text{nonzero finite}$ $\tilde{Q}, \tilde{q} \rightarrow 0$	$\tilde{E}, \tilde{Q}, \tilde{e}, \tilde{q} \rightarrow 0$

TABLE II: Extreme values of the energy and the charge of Q-balls and Q-tubes in the V_3 model.

B. the V_4 model

Second, we consider another simple potential,

$$V_4(\phi) := \frac{m^2}{2}\phi^2 - \lambda\phi^4 + \frac{\phi^6}{M^2} \quad \text{with } m^2, \lambda, M^2 > 0, \quad (17)$$

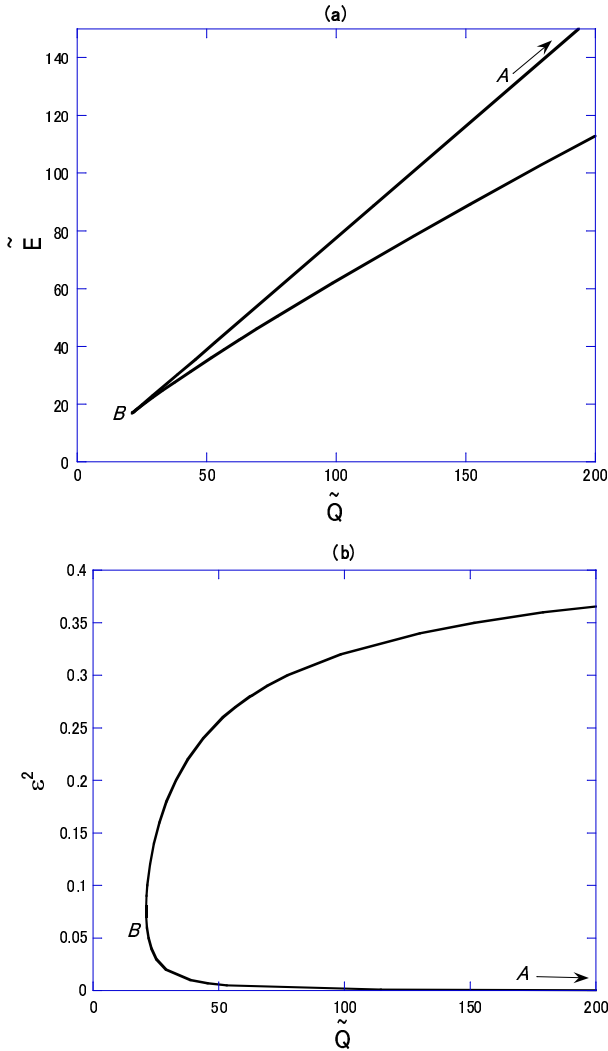


FIG. 7: (a) \tilde{Q} - \tilde{E} and (b) \tilde{Q} - $\tilde{\epsilon}^2$ relations for Type I Q-balls in the V_4 model: $\tilde{m}^2 = 0.6$.

which we call the V_4 model. We rescale the quantities as

$$\begin{aligned} \tilde{\phi} &\equiv \frac{\phi}{\sqrt{\lambda M}}, & \tilde{m} &\equiv \frac{m}{\lambda M}, & \tilde{\omega} &\equiv \frac{\omega}{\lambda M}, \\ \tilde{r} &\equiv \lambda M r, & \tilde{E} &\equiv \frac{E}{M}, & \tilde{Q} &\equiv \lambda Q, \\ \tilde{R} &\equiv \lambda M R, & \tilde{e} &\equiv \frac{e}{\lambda M^2} & \tilde{q} &\equiv \frac{q}{M}, \end{aligned} \quad (18)$$

and again define a parameter ϵ by (15).

Then the existing condition is identical to (16) in the V_3 case. We show the charge-energy- ϵ relations in Figs. 7-10: Type I Q-balls in Fig. 7, Type I Q-tubes in Fig. 8, Type II Q-balls in Fig. 9, and Type II Q-tubes in Fig. 10. Contrary to the case of the V_3 model, qualitative difference between Q-tubes and Q-balls appears. The extreme values of the energy and the charge of Q-balls and Q-tubes in the V_4 model are summarized in Table III.

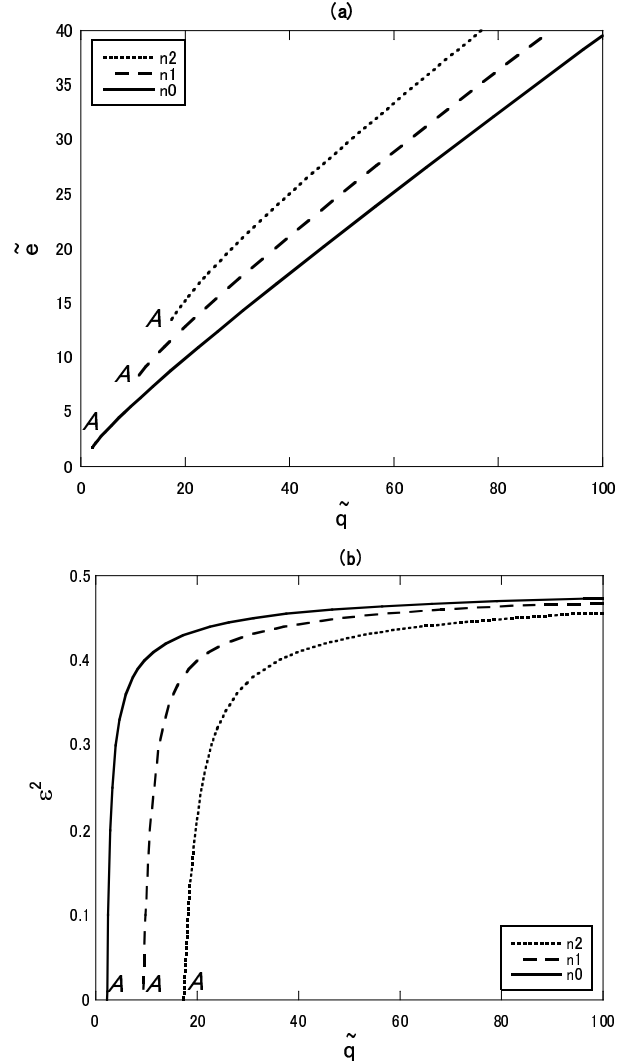


FIG. 8: (a) \tilde{q} - \tilde{e} and (b) \tilde{q} - $\tilde{\epsilon}^2$ relations for Type I Q-tubes in the V_4 model: $\tilde{m}^2 = 0.6$.

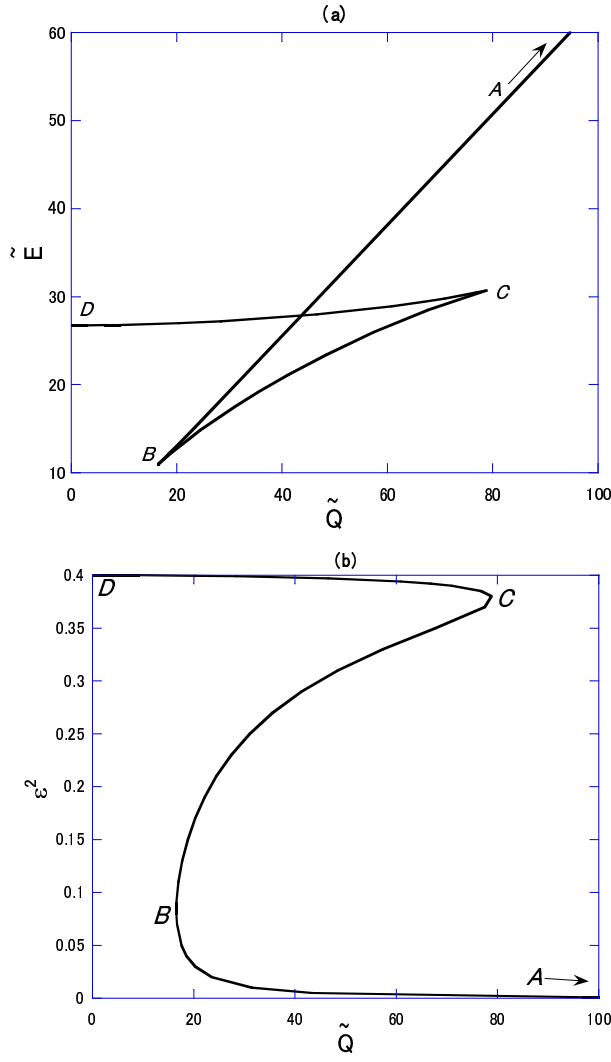


FIG. 9: (a) \tilde{Q} - \tilde{E} and (b) \tilde{Q} - ϵ^2 relations for Type II Q-balls in the V_4 model: $\tilde{m}^2 = 0.4$.

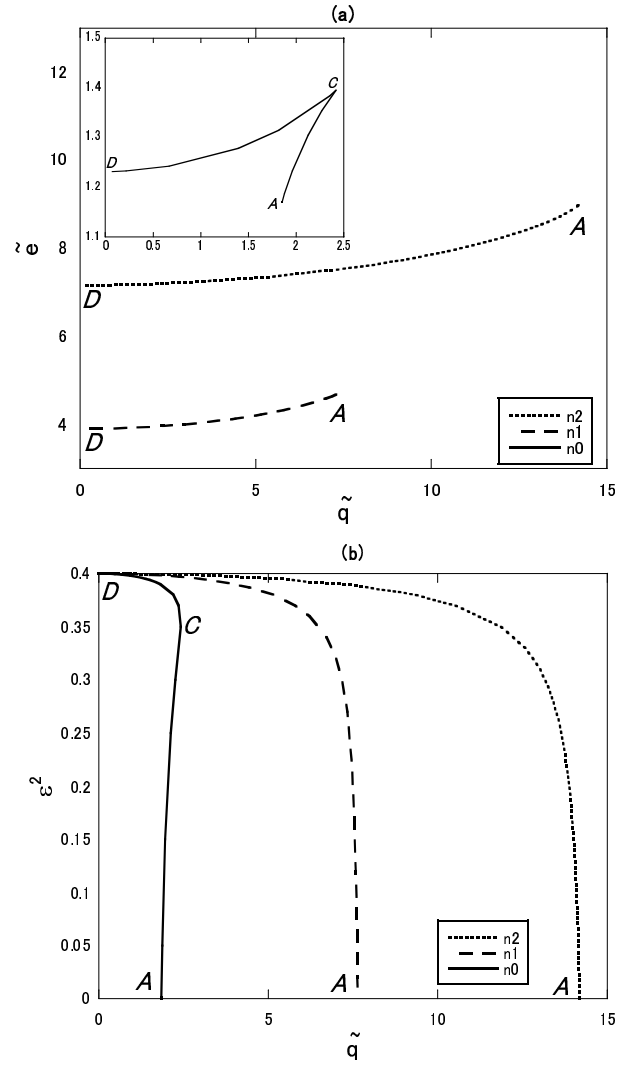


FIG. 10: (a) \tilde{q} - \tilde{e} and (b) \tilde{q} - ϵ^2 relations for Type II Q-tubes in the V_4 model: $\tilde{m}^2 = 0.4$.

	$\epsilon^2 \rightarrow \min[1/2, \tilde{m}^2]$	$\epsilon^2 \rightarrow 0$ (thick)
Type I: $\tilde{m}^2 > 1/2$	$\tilde{E}, \tilde{Q}, \tilde{e}, \tilde{q} \rightarrow \infty$	$\tilde{E}, \tilde{Q} \rightarrow \infty$ $\tilde{e}, \tilde{q} \rightarrow \text{nonzero finite}$
Type II: $\tilde{m}^2 < 1/2$	$\tilde{E}, \tilde{e} \rightarrow \text{nonzero finite}$ $\tilde{Q}, \tilde{q} \rightarrow 0$	$\tilde{E}, \tilde{Q} \rightarrow \infty$ $\tilde{e}, \tilde{q} \rightarrow \text{nonzero finite}$

TABLE III: Extreme values of the energy and the charge of Q-balls and Q-tubes in the V_4 model.

The structures of the solution series of Type II Q-balls and Q-tubes are not simple. In the case of Q-balls, there are two cusps in the Q - E diagram, B and C . Only the solutions between these two points represent stable solutions. In the case of Q-tubes, a cusp appears for $n = 0$, while no cusp appears for $n \geq 1$.

C. AD gravity-mediation type

From the theoretical point of view, it is important to investigate Q-tubes as well as Q-balls in the AD mechanism. There are two types of potentials: gravity-mediation type and gauge-mediation type. Here we consider the former type,

$$V_{\text{grav.}}(\phi) := \frac{m_{\text{grav.}}^2}{2} \phi^2 \left[1 + K \ln \left(\frac{\phi}{M} \right)^2 \right]$$

with $m_{\text{grav.}}^2, M > 0$. (19)

We rescale the quantities as

$$\tilde{\phi} \equiv \frac{\phi}{M}, \quad \tilde{\omega} \equiv \frac{\omega}{m_{\text{grav.}}},$$

$$\tilde{r} \equiv m_{\text{grav.}} r, \quad \tilde{E} \equiv \frac{m_{\text{grav.}} E}{M^2}, \quad \tilde{Q} \equiv \frac{m_{\text{grav.}}^2 Q}{M^2},$$

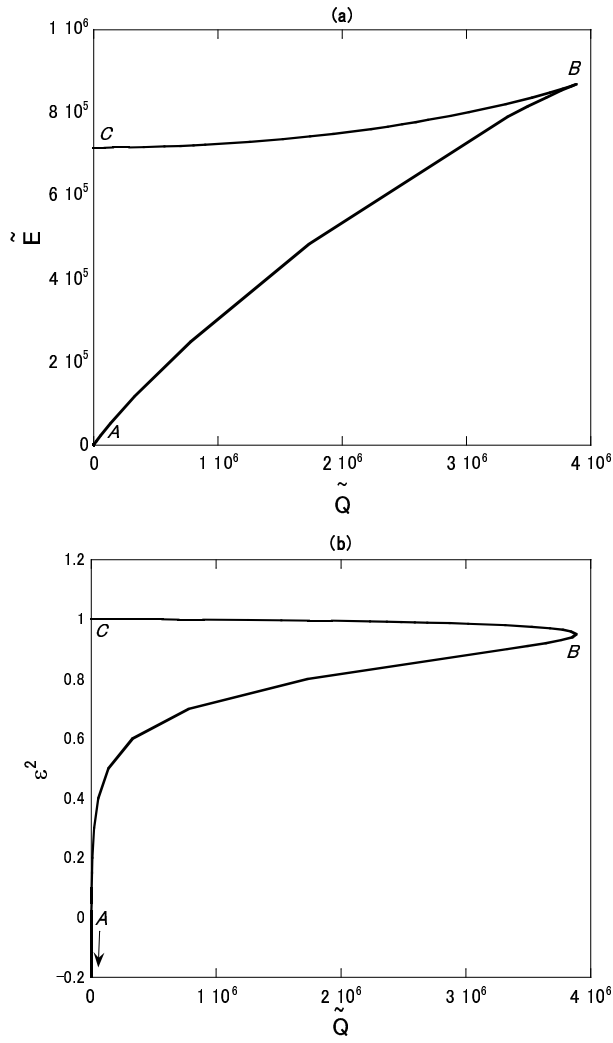


FIG. 11: (a) \tilde{Q} - \tilde{E} and (b) \tilde{Q} - ϵ^2 relations for $V_{\text{grav.}}$: $K = -0.1$.

$$\tilde{R} \equiv m_{\text{grav.}} R, \quad \tilde{e} \equiv \frac{e}{M^2}, \quad \tilde{q} \equiv \frac{m_{\text{grav.}} q}{M^2}, \quad (20)$$

and define a parameter ϵ as

$$\epsilon^2 = 1 - \tilde{\omega}^2. \quad (21)$$

The existing condition (7) becomes

$$K < 0, \quad \epsilon^2 < 1. \quad (22)$$

Thus, ϵ^2 is not bounded below, which is in contrast to the V_3 and V_4 models. Only Type II solutions exist in this model unless we introduce additional terms in the potential. We show the charge-energy- ϵ relations: Q-balls in Fig. 11 and Q-tubes in Fig. 12. The extreme values of the energy and the charge of Q-balls and Q-tubes in the gravity-mediation type are summarized in Table IV. There is no qualitative difference in the charge-energy relation between Q-balls and Q-tubes. These properties are common to Type II solutions in the V_3 model.

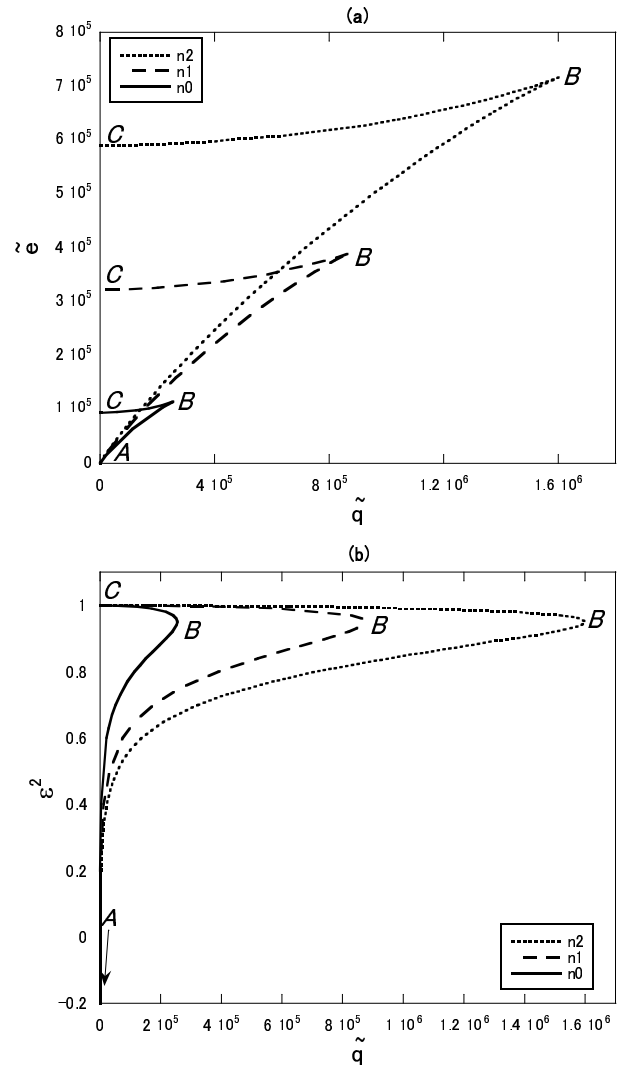


FIG. 12: (a) \tilde{q} - \tilde{e} and (b) \tilde{q} - ϵ^2 relations for $V_{\text{grav.}}$: $K = -0.1$.

	$\epsilon^2 \rightarrow 1$	$\epsilon^2 \rightarrow -\infty$ (thick)
Type II	$\tilde{E}, \tilde{e} \rightarrow \text{nonzero finite}$	$\tilde{E}, \tilde{Q}, \tilde{e}, \tilde{q} \rightarrow 0$
	$\tilde{Q}, \tilde{q} \rightarrow 0$	

TABLE IV: Extreme values of the energy and the charge of Q-balls and Q-tubes in the AD gravity-mediation type.

D. AD gauge-mediation type

Finally, we consider the gauge-mediation type in the AD mechanicsm,

$$V_{\text{gauge}}(\phi) := m_{\text{gauge}}^4 \ln \left(1 + \frac{\phi^2}{m_{\text{gauge}}^2} \right) \quad \text{with} \quad m_{\text{gauge}}^2 > 0. \quad (23)$$

We rescale the quantities as

$$\tilde{\phi} \equiv \frac{\phi}{m_{\text{gauge}}}, \quad \tilde{\omega} \equiv \frac{\omega}{m_{\text{gauge}}},$$

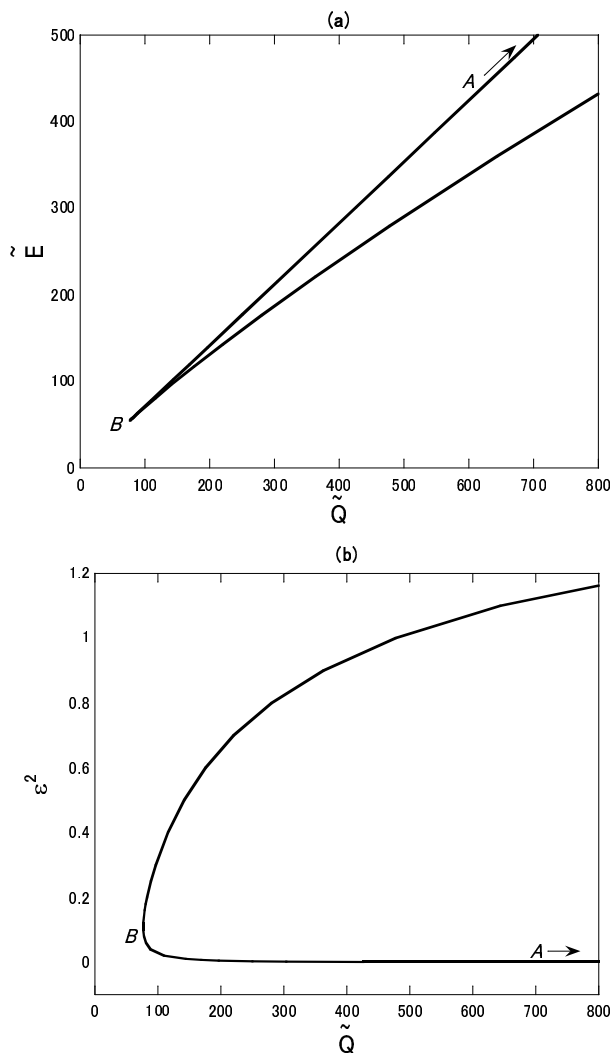


FIG. 13: (a) \tilde{Q} - \tilde{E} and (b) \tilde{Q} - $\tilde{\epsilon}^2$ relations for V_{gauge} .

$$\begin{aligned} \tilde{r} &\equiv m_{\text{gauge}} r, & \tilde{E} &\equiv \frac{E}{m_{\text{gauge}}}, & \tilde{Q} &\equiv Q, \\ \tilde{R} &\equiv m_{\text{gauge}} R, & \tilde{\epsilon} &\equiv \frac{\epsilon}{m_{\text{gauge}}^2}, & \tilde{q} &\equiv \frac{q}{m_{\text{gauge}}}, \end{aligned} \quad (24)$$

and define a parameter ϵ as

$$\epsilon^2 = 2 - \tilde{\omega}^2. \quad (25)$$

Then the existing condition (7) becomes

$$0 < \epsilon^2 < 2. \quad (26)$$

Only Type I solutions exist in this model. We show the charge-energy- ϵ relation: Q-balls in Fig. 13 and Q-tubes in Fig. 14. The extreme values of the energy and the charge of Q-balls and Q-tubes in the gravity-mediation type are summarized in Table V. These properties are common to the Type I solutions in the V_4 model.

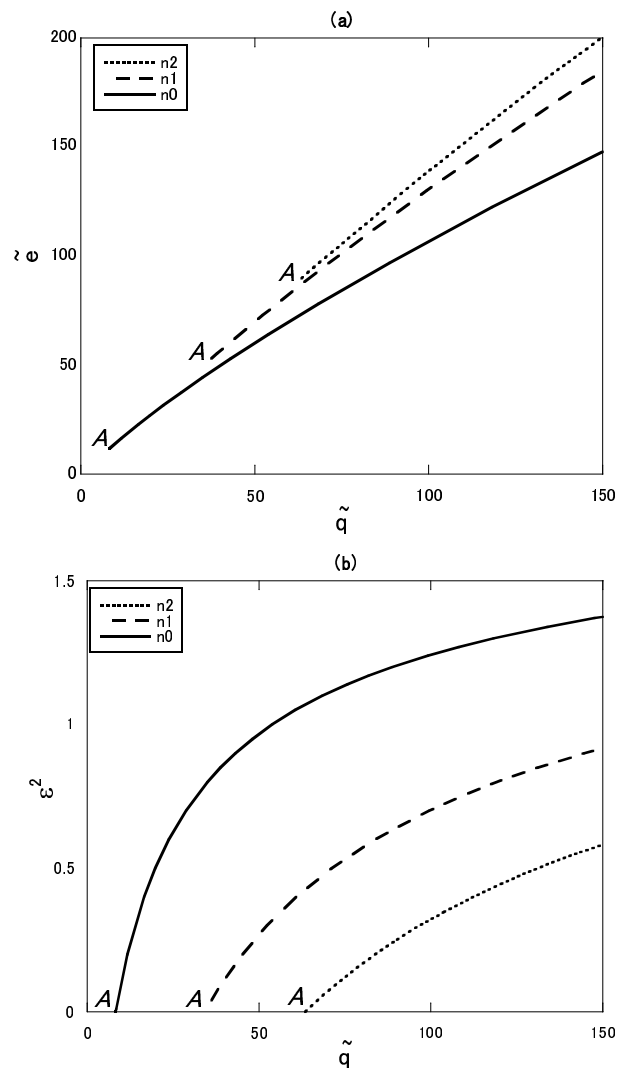


FIG. 14: (a) \tilde{q} - $\tilde{\epsilon}$ and (b) \tilde{q} - $\tilde{\epsilon}^2$ relations for V_{gauge} .

	$\epsilon^2 \rightarrow 2$ (thin)	$\epsilon^2 \rightarrow 0$ (thick)
Type I	$\tilde{E}, \tilde{Q}, \tilde{\epsilon}, \tilde{q} \rightarrow \infty$	$\tilde{E}, \tilde{Q} \rightarrow \infty$ $\tilde{\epsilon}, \tilde{q} \rightarrow \text{nonzero finite}$

TABLE V: Extreme values of the energy and the charge of Q-balls and Q-tubes in the AD gauge-mediation type.

IV. UNIFIED PICTURE OF Q-BALLS AND Q-TUBES

Our numerical results in the last section indicate that the charge-energy relation of equilibrium solutions depends a great deal on functional forms of the potential $V(\phi)$. In this section we discuss what determines the extreme values of the energy and the charge by analytical methods. As we explained in Sec. II, we can understand Q-balls and Q-tubes in words of a particle motion in Newtonian mechanics. In Fig. 1, if we ignore ‘non conserved force’ the maximum of ϕ , ϕ_{max} , is determined by

the nontrivial solution of $V_\omega = 0$. Using this $\tilde{\phi}_{\max}$, we can evaluate the order of magnitude of the energy and the charge, (8) and (13), as

$$\begin{aligned}\tilde{E} &\sim \tilde{r}_{\max}^3 \left\{ \frac{1}{2} \tilde{\omega}^2 \tilde{\phi}_{\max}^2 + \frac{1}{2} \left(\frac{d\tilde{\phi}}{d\tilde{r}} \right)^2 + \tilde{V} \right\}, \\ \tilde{Q} &\sim \tilde{\omega} \tilde{r}_{\max}^3 \tilde{\phi}_{\max}^2, \\ \tilde{e} &\sim \tilde{R}_{\max}^2 \left\{ \frac{1}{2} \tilde{\omega}^2 \tilde{\phi}_{\max}^2 + \frac{1}{2} \left(\frac{d\tilde{\phi}}{d\tilde{R}} \right)^2 + \frac{n^2 \tilde{\phi}_{\max}^2}{2\tilde{R}_{\max}^2} + \tilde{V} \right\}, \\ \tilde{q} &\sim \tilde{\omega} \tilde{R}_{\max}^2 \tilde{\phi}_{\max}^2,\end{aligned}\quad (27)$$

where the subscript ‘‘max’’ denote the values at which $\tilde{\phi} = \tilde{\phi}_{\max}$. As for \tilde{R}_{\max} for $n = 0$ or \tilde{r}_{\max} , it is reasonable to take \tilde{R} or \tilde{r} where $\tilde{\phi}$ becomes about $0.5\tilde{\phi}_{\max}$.

What we want to discuss is whether \tilde{E} , \tilde{Q} , \tilde{e} and \tilde{q} approach zero, infinity or nonzero finite values as ϵ^2 approaches the upper or lower limit. The approximate expression (27) is appropriate for this purpose.

First, we discuss the upper limit of ϵ^2 , or equivalently, the lower limit of ω^2 . In Type I solutions, where $\min[V] = V(0) = 0$, in the limit of $\omega \rightarrow \min[2V/\phi^2]$, the minimum of V_ω approaches zero. In this case, in the Newtonian-mechanics picture of Fig. 1, a particle rolls down from the top of the hill over infinite time, i.e., R_{\max} diverges. This limit corresponds to the thin-wall limit. From the expression (27), we see that \tilde{Q} , \tilde{E} , \tilde{q} and \tilde{e} diverge.

On the other hand, in the Type II solutions, where $\min[V] < 0$, because $V_\omega < V$, there is no limit of $\min V_\omega \rightarrow 0$. Therefore, \tilde{Q} , \tilde{E} , \tilde{q} and \tilde{e} must have their upper limits.

Next, we investigate the lower limit of ϵ^2 , or equivalently, the upper limit of ω^2 . This limit corresponds to the thick-wall limit. Except for the $V_{\text{grav.}}$ model, ϵ satisfies

$$\epsilon^2 = \frac{1}{m^2} \frac{d^2 V_\omega}{d\phi^2}(0), \quad (28)$$

which means that ϵ is the mass scale of V_ω normalized by m . Therefore, the wall thickness normalized by m is of order of $1/\epsilon$. Because the radius and the wall thickness are of the same order in the thick-wall limit, except for the $V_{\text{grav.}}$ model, we obtain

$$\tilde{r}_{\max}, \tilde{R}_{\max} \sim \frac{1}{\epsilon}. \quad (29)$$

In the following, from the approximate expression (27) and (29) we evaluate the limits of the charge and the energy as ϵ approaches the lower limit.

(A) V_3 case

The solution of $V_\omega = 0$ is

$$\tilde{\phi}_{\max} = \frac{1 - \sqrt{1 - 2\epsilon^2}}{2}. \quad (30)$$

In the lower limit $\epsilon^2 \rightarrow 0$, we have $\tilde{\phi}_{\max} \simeq \epsilon^2/2$. Therefore, from (27)-(29), we find

$$\tilde{Q}, \tilde{E}, \tilde{q}, \tilde{e} \rightarrow 0, \quad (31)$$

which agree with the numerical results in Table II.

(B) V_4 case

From $V_\omega = 0$, we obtain

$$\tilde{\phi}_{\max}^2 = \frac{1 - \sqrt{1 - 2\epsilon^2}}{2}. \quad (32)$$

In the lower limit $\epsilon^2 \rightarrow 0$, we have $\tilde{\phi}_{\max} \simeq \epsilon$. Substituting this and (29) into (27), we have

$$\begin{aligned}\tilde{E} &\sim \frac{1}{\epsilon^3} \frac{1}{2} \tilde{\omega}^2 \epsilon^2 \rightarrow \infty, & \tilde{Q} &\sim \tilde{\omega} \frac{1}{\epsilon^3} \epsilon^2 \rightarrow \infty, \\ \tilde{e} &\sim \frac{1}{\epsilon^2} \frac{1}{2} \tilde{\omega}^2 \epsilon^2 \rightarrow \text{const.}, & \tilde{q} &\sim \tilde{\omega} \frac{1}{\epsilon^2} \epsilon^2 \rightarrow \text{const.},\end{aligned}\quad (33)$$

which agree with the numerical results in Table III. This explains why the results between Q-tubes and Q-balls are different in this model while no qualitative difference appears in the V_3 model.

(C) $V_{\text{grav.}}$ case

The solution of $V_\omega = 0$ is

$$\tilde{\phi}_{\max} = e^{-\frac{\epsilon^2}{2\kappa}}. \quad (34)$$

We note that dependence on K is extremely large. $\tilde{\phi}_{\max}$ approaches zero in the lower limit $\epsilon^2 \rightarrow -\infty$. Since R_{\max} does not diverge,

$$\tilde{Q}, \tilde{E}, \tilde{q}, \tilde{e} \rightarrow 0, \quad (35)$$

which agree with the numerical results in Table IV.

In a realistic situation, we anticipate that $V_{\text{grav.}}$ has also the nonrenormalization term $\tilde{V}_{\text{NR}} = \beta\tilde{\phi}^n$ where $\beta > 0$ and $n > 2$. This does not change the qualitative behavior in the lower limit. However, in the upper limit, $V_\omega = 0$ has degenerate solutions as in Type I models. Therefore, we anticipate that the charge-energy relation for $V_{\text{grav.}}$ with \tilde{V}_{NR} is similar to that for Type I solutions in the V_3 model.

(D) V_{gauge} case

We should solve

$$\ln(1 + \tilde{\phi}_{\max}^2) = \frac{\tilde{\omega}^2 \tilde{\phi}_{\max}^2}{2}. \quad (36)$$

In the lower limit $\epsilon^2 \rightarrow 0$, if we use Maclaurin expansion and neglect higher order terms $O(\tilde{\phi}_{\max}^5)$, we have

$$\tilde{\phi}_{\max}^2 \epsilon^2 \simeq \tilde{\phi}_{\max}^4. \quad (37)$$

Then, we obtain

$$\tilde{\phi}_{\max} \simeq \epsilon, \quad (38)$$

as in the V_4 model. Therefore, the limit values are identical to (33), which agree with the numerical results in Table V. We also understand why the results for V_4 with $\tilde{m}^2 > 1/2$ and for V_{gauge} are qualitatively the same.

V. SUMMARY AND DISCUSSIONS

We have made a comparative study of Q-balls and Q-tubes. First, we have investigated their equilibrium solutions for four types of potentials. The charge-energy relation depends on potential models. We have also noted that in some models the charge-energy relation is similar between Q-balls and Q-tubes while in other models the relation is quite different between them. To understand what determines the charge-energy relation, which is a key of stability of the equilibrium solutions, we have established an analytical method to obtain the two limit values of the energy and the charge. Our results have

indicated how the existent domain of solutions and their stability depends on their shape as well as potentials. This method would also be useful for other Q-objects or those in higher-dimensional spacetime. These are our next subjects.

Acknowledgments

We would like to thank Kei-ichi Maeda for continuous encouragement. The numerical calculations were carried out on SX8 at YITP in Kyoto University.

-
- [1] A. Kusenko, Phys.Lett. B 405, 108 (1997) 108; Nucl. Phys. B (Proc. Suppl.) 62A-C, 248 (1998).
 - [2] I. Affleck and M. Dine, Nucl. Phys. B **249** 361 (1985).
 - [3] K. Enqvist and J. McDonald, Phys. Lett. B **425**, 309 (1998); Nucl. Phys. B **538**, 321 (1999); S. Kasuya and M. Kawasaki, Phys. Rev. D **62**, 023512 (2000).
 - [4] A. Kusenko and M. Shaposhnikov, Phys. Lett. B **418**, 46 (1998); I. M. Shoemaker and A. Kusenko, Phys. Rev. D **80**, 075021 (2009).
 - [5] A. Kusenko *et al.* Phys. Lett. B **423** 104, (1998).
 - [6] A. Kusenko, Phys. Lett. B **404**, 285 (1997); **406**, 26 (1997); T. Multamaki and I. Vilja, Nucl. Phys. B **574**, 130 (2000); M. Axenides, S. Komineas, L. Perivolaropoulos and M. Floratos, Phys. Rev. D **61**, 085006 (2000); M. I. Tsumagari, E. J. Copeland, and P. M. Saffin, *ibid.* **78**, 065021 (2008).
 - [7] F. Paccetti Correia and M. G. Schmidt, Eur. Phys. J. **C21**, 181 (2001).
 - [8] N. Sakai and M. Sasaki, Prog. of Theor. Phys., **119**, 929 (2008).
 - [9] T. Tamaki and N. Sakai, Phys. Rev. D **81**, 124041 (2010); *ibid.* **83**, 044027 (2011); *ibid.* **83**, 084046 (2011); *ibid.* **84**, 044054 (2011).
 - [10] For a review, see, e.g., A. Vilenkin and E.P.S. Shellard, *Cosmic Strings and Other Topological Defects*, Cambridge (1994).
 - [11] N. Sakai, H. Ishihara and K. Nakao, Phys. Rev. D **84**, 105022 (2011).
 - [12] K. Enqvist and A. Jokinen, T. Multamaki, and I. Vilja, Phys. Rev. D, **63**, 083501 (2001); E.J. Copeland and M.I. Tsumagari, *ibid.* **80**, 025016 (2009); T. Hiramastu, M. Kawasaki, and F. Takahashi, JCAP **06**, 008 (2010).
 - [13] R. Battye and Paul Sutcliffe, Nucl. Phys. B **590** 329 (2000); M.I. Tsumagari, <http://www.nottingham.ac.uk/~ppzphy7/webpages/people/Mitsuo/welcome.html>
 - [14] M.I. Tsumagari, E.J. Copeland, and P.M. Saffin, Phys. Rev. D **78**, 065021 (2008).
 - [15] S. Coleman, Nucl. Phys. **B262**, 263 (1985).
 - [16] Y. Kim, K. Maeda, and N. Sakai, Nucl. Phys. **B481** 453, (1996); Y. Kim, S. J. Lee, K. Maeda, and N. Sakai, Phys. Lett. B **452**, 214 (1999).
 - [17] For a review of catastrophe theory, see, e.g., T. Poston and I.N. Stewart, *Catastrophe Theory and Its Application*, Pitman (1978).